



POLITECNICO
MILANO 1863

SCUOLA DI INGEGNERIA INDUSTRIALE
E DELL'INFORMAZIONE

EXECUTIVE SUMMARY OF THE THESIS

Characterisation of the properties of creases in thin Kapton sheets for the realisation of a drag sail

LAUREA MAGISTRALE IN SPACE ENGINEERING - INGEGNERIA SPAZIALE

Author: SIMONE ZAPPELLA

Advisor: PROF. ANTONIO MATTIA GRANDE

Co-advisor: FILIPPO CARNIER

Academic year: 2023-2024

1. Introduction

In 1957 the first satellite was sent into orbit around Earth and, from that moment, the number of man-made objects orbiting around Earth has constantly increased. In the beginning, this wasn't considered a problem, but with the years passing by the uncontrolled artificial bodies in orbit grew in number, and with it the danger of impacts between uncontrolled bodies, commonly called space debris, and operative satellites, causing the formation of new debris with the Kessler effect. The first regulations on the topic were defined in 2001, imposing that new satellites and parts of launchers in Low Earth Orbit shall be deorbited in 25 years, but a tightening was made in 2022 to reduce this period to 5 years [1], as a proof of the importance of the phenomena. The deorbit can be achieved by using classical propulsion or other, such as the emerging technology of drag sails, which generate the deorbiting force relying on atmospheric drag and solar radiation pressure. Both these effects depend on the area of the sail, therefore these devices need to have a big area, but before activation, they need to be stored in a limited space on the fairing of the launcher, and here the origami technology comes extremely useful,

consenting to achieve the packaging of the sail by occupying a low volume. For the design of origami and to simulate its behaviour numerically is necessary the knowledge of its properties. In particular, the properties of the creases need to be determined to regulate the unfolding and design the actuators. The sail designed in this work is composed of Dupont™ Kapton HN and actuated with a set of Shape Memory Alloy wires. The aim of this work is to determine the properties of the mentioned material so that they can be used in a numerical prediction of the unfolding of the sail.

2. Crease testing and modelling

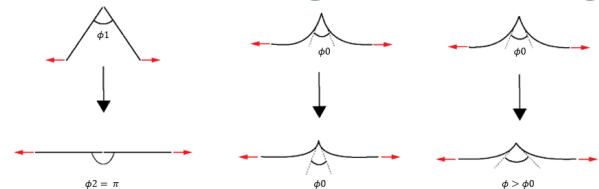


Figure 1: Possible behaviours of creases

An important feature of a crease is the neutral angle, indicated with Φ_0 , representing the angle at which the crease is at rest. For thin membranes composed of polymeric materials, the unfolding process is governed by a combination of elastic bending of the faces and deformation as-

sociated with the opening of the crease, as in Figure 1, which compare in different magnitudes depending on the material properties and faces length.

2.1. Experimental activity and tests

The material selected for the experimental investigation is a Kapton HN sheet produced by Dupont™. Two thicknesses were selected: 50.8 and 76.2 micrometres. The first operation carried out in the experimental activities is the bending of the samples: samples with a width of 25, 50 and 100 millimetres and face lengths of 29 millimetres each are cut to the designed dimensions, then adhesive tape is used to join and keep in position the sides of the samples that are then are placed between flat slabs and under a weight of 20 kilograms. Due to the viscoplastic nature of Kapton, simply placing the weights on the samples is not enough to obtain a low neutral angle, but according to [2] the pressing force has to be maintained for 2 hours. To obtain an even lower neutral angle, two samples were bent in an oven at a temperature of 120°C, using weights of 10 and 20 kilograms respectively. After the samples are folded, the neutral angle is expected to grow in time for the occurrence of viscoelastic effects following a logarithmic law: the relaxation of the angle is fast right after the bending process is concluded and gets slower as time passes by. For this reason, before proceeding with the tests, the samples rest for 24 hours. After this time is passed, the samples are placed unloaded on white paper with a graded scale, and pictures are taken to be used for the measurement of the neutral angle. The tests were performed on a Dynamic Mechanical Analyser (Anton Paar MCR 702e Multidrive), and the samples were mounted using 3D printed supports to adapt the width of the sample to the grips of the machine. After mounting the sample on the machine, this is brought to a gap of 28 millimetres, where for gap is intended the distance between the two ends of the free sample. This position is maintained for 30 seconds and then the gap is raised to a value of 53 millimetres with a velocity of 3 millimetres per second. During this process, pictures are taken with a Canon EOS 70D camera and used in the processing to determine the deformation of the sample along its profile. Three tests are conducted for almost all the analysed samples.

2.2. Analysis of the acquired data

The analysis of the data starts with the determination of the neutral angle using the pictures taken before the tests. Each image is processed with a digital image processing tool (*WebPlot-Digitizer*). The coordinates are then analysed in Matlab by representing them using an equation that reconstructs the shape of the profile using two parameters: the neutral angle and a representative length of the crease [3]. Using a shooting function these two parameters are found; an example is reported in Figure 2. Then all the

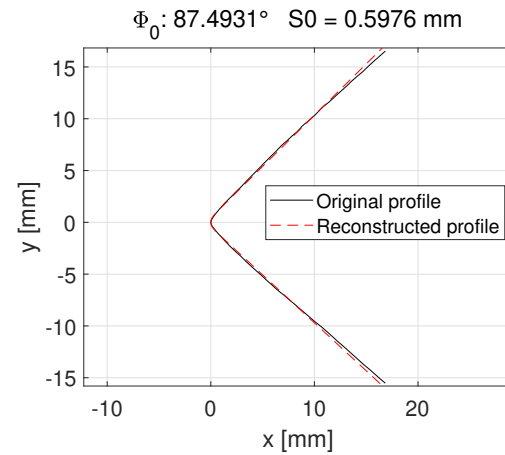


Figure 2: Reconstruction of the neutral angle

pictures taken during the tests are analysed with the same program and the shape of the deformed profile is acquired for every configuration. The

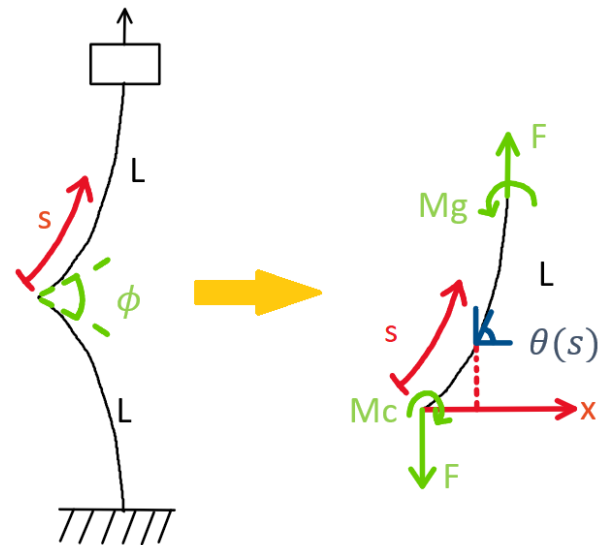


Figure 3: Model used to reconstruct the profile profile is modelled as depicted in Figure 3 and the angle θ is measured using simple goniometric relations. The force used to open the folded sheet, F , is measured by the DMA during the tests, the length of the faces of the profile, L ,

is known and the S coordinate is measured in Matlab exploiting the coordinates of the points. The moment in the grip, M_g , is not needed in the analysis and the crease moment, M_c , is to be determined.

$$\kappa(S) = \frac{d\theta(S)}{dS} = M(S) \frac{12(1-\nu^2)}{EWh^3} \quad (1)$$

$$M(S) = M_c - F \cdot x(S) \quad (2)$$

M_c is determined using a shooting algorithm: at first a guess is made and $M(S)$ is determined using Equation 2, then Equation 1 is reversed and the angle θ is determined relying on the just computed moment distribution along the profile. At last, an error is computed by evaluating the difference between the angle θ determined from the images and the one computed with the guessed parameters. Using the Matlab function *fminsearch*, the parameters that minimise the error are determined, following the procedure suggested by Dharmadasa [4]. The folding angle is then measured using the same method used to determine the neutral angle but limiting the research of the parameters to a region near the crease, up to a distance of 4 millimetres measured along S . According to the [4], the relationship between the folding angle and crease moment is linear and can be described using only one parameter, k , which represents the stiffness of the crease. This parameter is determined using a linear regression that, for all the tests, has a value of R^2 of at least 95%. The results are

h [μm]	k [$\text{N}/^\circ$]	95% confidence level
50.8	0.000148	0.00001006
76.2	0.000847	0.00005904

Table 1: Resultant values of crease stiffness

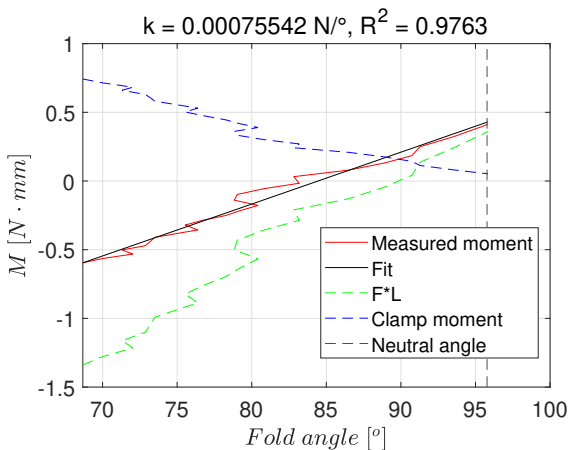


Figure 4: Example of results for a 76.2 μm thick sample

then analysed using a t-student distribution, and the variability of the results is computed using a confidence level of 95%. The results of this analysis are reported in Table 1.

An example of the results of a single test is reported in Figure 4, where the raw data and the performed fitting are reported. It's also visible that the crease moment goes to zero at an angle different from the neutral angle determined using the picture of the unloaded sample, a common occurrence in the analysis of the results.

3. Characterisation of the viscoelastic properties of Kapton

Kapton is a viscoplastic material, but due to the low forces experienced by the samples during the tests, it can be modelled as simply viscoelastic without committing any errors. After a careful analysis of the existing viscoelastic models and also considering how Abaqus, used in Section 4, works, it is decided to represent the viscoelastic model using a Prony Series, in Equation 3, which in turn can be referred to the Wiechert model, shown in Figure 5, where the material is modelled as a series of springs and dumpers.

$$E(t) = \sum_{i=1}^n E_i \cdot e^{-t/\tau_i} + E_\infty \quad (3)$$

From the coefficient expressed in the figure, the Prony series is composed knowing that the relaxation time is computed in this way: $\tau_i = \mu_i/E_i$. For the characterisation of the viscoelastic pa-

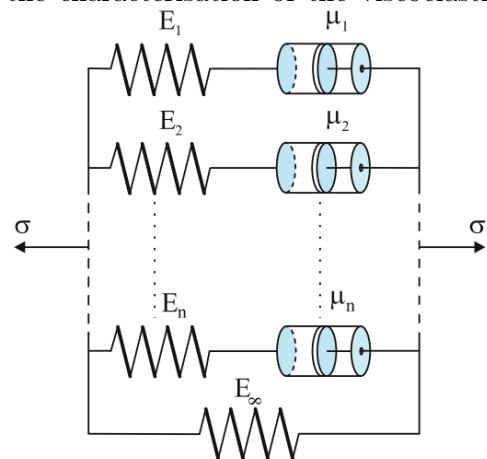


Figure 5: Wiechert viscoelastic model parameters, it is decided to proceed using a particular kind of creep test: the Stepped Isothermal Method (SIM). In a classical creep test, a defined load is applied to the specimen and maintained in time, and keeping a constant stress the strain is expected to rise in time. Using the SIM

the sample undergoes a predetermined number of creep steps in series, at defined temperatures: the designed load is applied at the first temperature and maintained for the required time, and then the temperature is raised as quickly as possible to the next designed temperature and the second step begins, and so on. All the steps have the same duration and in the whole process the load is never released until the end, consenting to automate a procedure that classically is particularly time-consuming, in which the different creep tests are run separately. The data are then analysed using the Time-Temperature Superposition Principle (TTSP) [5], which expresses the relation, present in polymers, between the temperature and the creep velocity, that rises with the temperature. Following this principle, the data are converted from a measure of strain to an elastic modulus and rescaled in the time domain to form a mastercurve. The SIM test was actuated on samples with dimensions of 13X42 millimetres, but considering the length of the grips, the free length of the sample is of 30 millimetres, while the steps followed are of 10000 seconds each at temperatures of 23, 30, 40, 50, 60, 70 and 80°C. Unfortunately, the machine used to perform the test was not optimal for this kind of application, starting from the limitations it gave to the dimensions of the samples, far less than what was advised by the standards, to the time required to perform the temperature steps, which was too elevated. Due to these factors, only one of the four SIM tests performed gives an acceptable mastercurve, and for this uncertainty, it was decided to not proceed with the data of the whole SIM test but to take only the data of the first creep step, long enough to simulate the tests of Section 2. The output of the first step of the tests is reported in Figure 6 for all the four tests performed, along with the mean response, which was then used to build the viscoelastic model. The determination of the model was made directly by building the Prony series, researching the values of five relaxation times, five elastic moduli related to the relaxation times, and E_∞ to complete the series, using a method divided into two phases. In the first phase a genetic algorithm was used to research in a limited range a good initial guess to feed in the second phase to a minimization algorithm. Genetic algorithms can find good pa-

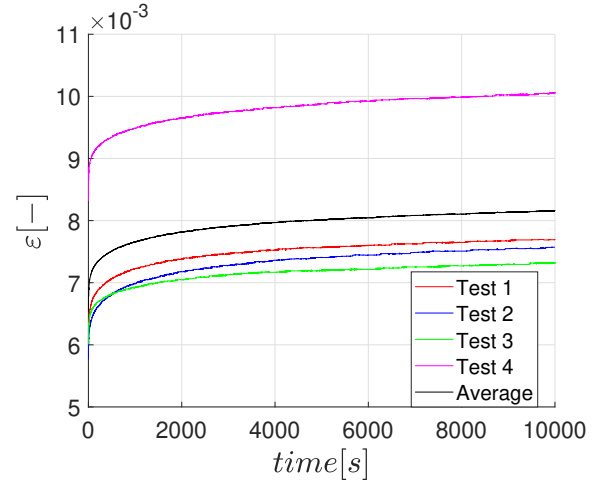


Figure 6: Strain obtained with 20 Newton load in the first SIM step

rameters in a given range, but they are chosen casually and evaluated using an error function, that's why the minimization process is necessary after this step. The final coefficients are reported

τ [s]	E_i [MPa]	E_i/E_0 [-]
0.573	677.59	0.18572
15.597	90.253	0.024737
105.996	110.1	0.030176
897.041	167.49	0.045905
7811.255	177.06	0.04853
$E_\infty = 2426.06$ MPa		
$E_0 = 3648.55$ MPa		

Table 2: Coefficients of the Prony series

in Table 2 along with E_0 , equal to the value of the elastic modulus at $t = 0$. The confrontation

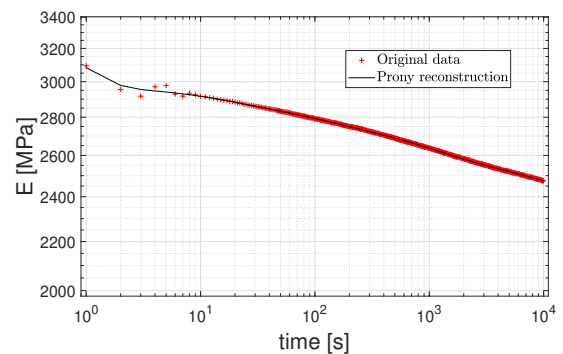


Figure 7: Confrontation test data - model

between the original data and the reconstruction actuated with the Prony series is shown in Figure 7, where it can be seen that the model can successfully predict the results of the tests.

4. Numerical simulations

After the characterisation of the properties of the material is complete, numerical simulations are made to check if the determined parameters can reconstruct the results of the tests. Since the crease was represented in Section 2 as a torsional spring, the most logical action would be to model it as a series of springs linked to the elements constituting the crease in the finite element model, but this operation is highly time-consuming and if springs are not placed in all the nodes may cause local effects. The solution

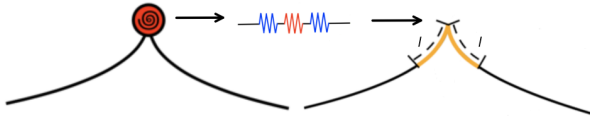


Figure 8: Adopted crease model

adopted to solve this problem is to model the crease as a partition of material with different properties determined by considering the crease as a series of three springs as in Figure 8, where the stiffness of the central spring is the one determined for the crease only and the other two represent the bending stiffness of a short part of the faces, computed with Equation 4.

$$M_b = \frac{Eh^3}{12(1-\nu^2)l} \Delta\theta = k_{shell} \Delta\theta \quad (4)$$

The equivalent stiffness of the crease is computed and then converted in a variation of the thickness (h) of the material constituting the crease reversing the equation, where l is the length of the partition indicated in Figure 8, E the elastic modulus and ν the Poisson ratio.

4.1. Parametric analysis

Before performing the final simulations a parametric analysis is performed. The reference used is a sample with a neutral angle of 100° , width of 10 millimetres, rot is 90° , $50.8 \mu m$ thickness and the correspondent mean stiffness. The force reported in the second image of Figure 9 is the result of the simulation made with these data. In the figure are also reported the parameters whose variation was analysed and the effect that the raising of each of them has on the gap-pulling force plot. The rotation of the relation due to a raising of the stiffness is centred on the level of gap where the crease moment is equal to zero, while for the thickness the rotation is centred at the gap where the pulling force is equal to zero.

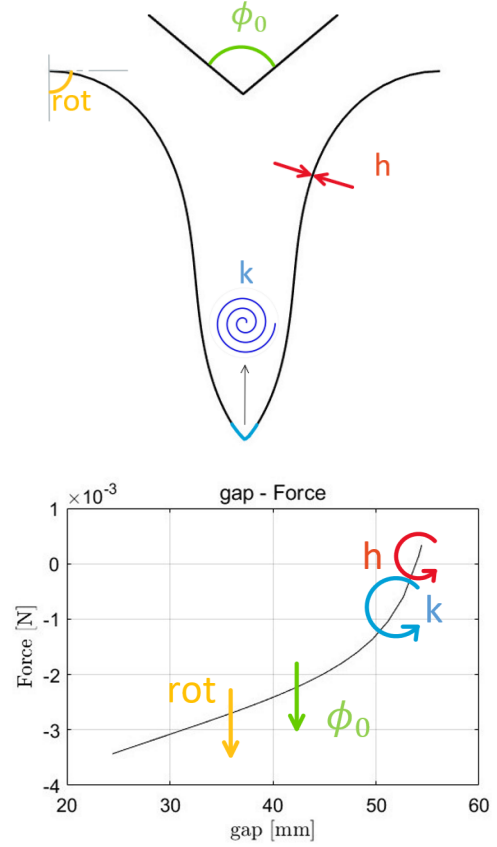


Figure 9: Parametric analysis

4.2. Final simulations

For every tested sample some numerical simulations were performed to compare real and simulated results, and the parametric analysis was exploited to vary the parameters and try to obtain a better response similarity. An example is

	$\Phi_0 [^\circ]$	$k [N/^\circ]$	$h [\mu m]$	$rot [^\circ]$
Original	114.6	$8.47 \cdot 10^{-4}$	76.2	90
Final	105	$8.02 \cdot 10^{-4}$	86	85

Table 3: Data used in the example

reported in Figure 10, where the meaning of the lines is explained in the caption and the force computed using the images was determined by upgrading the shooting algorithm described in Section 2. The example reported is representative of the 10 samples that were tested and analysed: it can be seen that the simulations performed with the initial (theoretical) data don't follow the response measured in the tests, but there is a good agreement with the response determined using only the images. On the other hand, varying the parameters of the simulation as in Table 3, the original response in most cases can be reconstructed, even if the final parameters are too far from the theoretical values to be physically sensed and realistic, concluding that

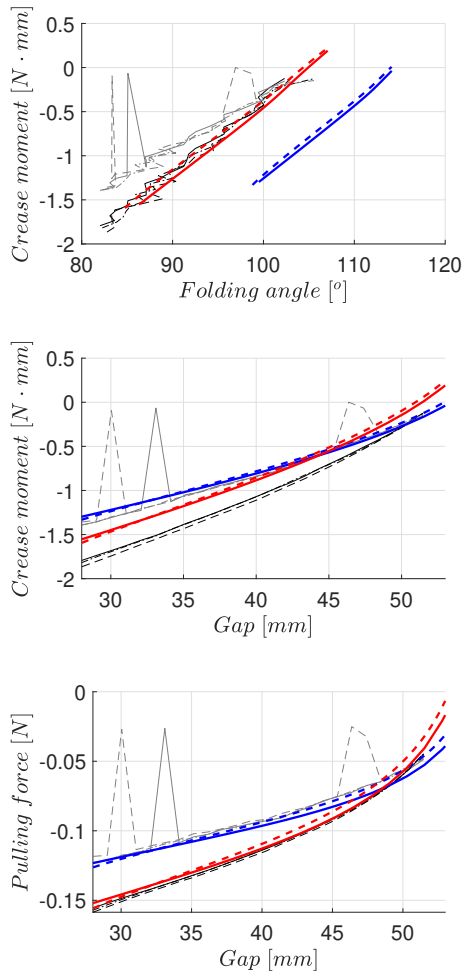


Figure 10: Results of the sample D75_100_1. Black lines: response from forces measured in the tests. Grey lines: response from forces computed using the pictures. Blue lines: response from simulations with original data. Red lines: response from simulations with final data. For coloured lines: full line = hyperelastic model, dashed line = viscoelastic model

these variations don't explain successfully the incongruences between tests and simulations. Another observation to be made is that, by using hyperelastic or viscoelastic models, the response computed numerically changes only in minor part, probably due to the low velocity in which the tests are performed. Looking at the results of the simulations and considering that most of the used Kapton sheets have irregular shapes, it was decided to perform a last set of simulations to compare the force needed to unfold a sample with straight faces with the forces used to unfold samples with curved faces. The result is that the magnitude of the variation of the pulling force is comparable to the distance present between the response of the original simulation and the test data, giving a possible candidate on the reason

that stays behind the incongruence between the test forces and the results of the simulations.

5. Conclusions

The characterisation of the stiffness of creases in Dupont™Kapton HN was carried out for sheets with two different thicknesses with good agreement between the results of different tests. Then the characterisation of the material continued with the determination of the viscoelastic properties through a series of creep tests at 23°C. At last, numerical simulations were carried out in Abaqus to validate the model, at first using the theoretical parameters and then adapting the values to attempt the reconstruction of the test data. In this last phase the test results are generally reconstructed, but the parameters used to obtain these results are usually particularly far from the theoretical values and deemed unrealistic. Observing the geometrical imperfections of the material, a last attempt is made to explain the incongruence of the results, simulating a profile with curved faces, finding that the difference between the force obtained in this way and the force coming from classical simulations with straight samples is comparable to the difference between the output of the tests and the result of the test simulations, giving credit to the characterisation process and to the model used to represent the crease.

References

- [1] FCC. *Space Innovation: Mitigation of Orbital Debris in the New Space Age*. 8 September 2022. FCC fact sheet.
- [2] Dharmadasa B. Yasara et al. "Formation of Plastic Creases in Thin Polyimide Films". In: *Journal of Applied Mechanics* 87 (2020).
- [3] Jules T., Lechenault F., and Adda-Bedia M. "Local Mechanical Description of an Elastic Fold". In: *Soft Matter* 15 (2019), pp. 1619–1626.
- [4] Dharmadasa B. Yasara and López Jiménez Francisco. "Modeling the Effects of Creases in an Unfolding Membrane". In: *AIAA Scitech Forum* (2021).
- [5] Brinson Hal F. and Brinson L. Catherine. *Polymer Engineering Science and Viscoelasticity, An introduction - Second edition*. Springer, 2015.